

Synthesis and characterization of novel poly(amide-ether)s bearing imidazole pendants: study of physical and optical properties

Mousa Ghaemy · Samaneh Sharifi ·
Seyed Mojtaba Amini Nasab · Mehdi Taghavi

Received: 1 May 2012 / Revised: 18 November 2012 / Accepted: 30 November 2012 /
Published online: 12 December 2012
© Springer-Verlag Berlin Heidelberg 2012

Abstract Two new *para*-linked diether-diamines, bis(4-(4-amino-2-(4,5-diphenyl-1H-imidazol-2-yl)phenoxy) phenyl)methanone and bis(4-(4-amino-2-(4,5-diphenyl-1H-imidazol-2-yl)phenoxy) phenyl)hexafluoropropane, bearing two *ortho*-linked phenyl-substituted imidazole pendants and trifluoromethyl groups were synthesized by the nucleophilic chlorodisplacement reaction of the synthesized 2-(2-chloro-5-nitrophenyl)-4,5-diphenyl-1H-imidazole with 4,4'-dihydroxybenzophenone or 4,4'-(hexafluoroisopropylidene)diphenol in refluxing DMAc in the presence of potassium carbonate. These diamines were utilized to prepare a series of novel poly(amide-ether)s (PAEs) via direct phosphorylation polycondensation with aliphatic and aromatic dicarboxylic acids. The polymeric samples were readily soluble in a variety of organic solvents and formed low-colored and flexible thin films via solution casting. These polymers showed glass-transition temperatures (T_g s) between 204 and 308 °C. Thermal behaviors of the PAEs were characterized by thermogravimetric analysis, and the 10 % weight loss temperatures were found to be in the range of 330–450 °C in N₂. The PAEs exhibited fluorescence emission in solution and in solid state with maxima around 423–494 nm and with the quantum yields in the range of 6–28 %.

Keywords Poly(amide-ether) · Direct polycondensation · Thermal properties · Fluorescent · Solubility

Introduction

Polyamides are one of the high-performance polymeric materials and are characterized by thermo-oxidative stability, good mechanical properties, and

M. Ghaemy (✉) · S. Sharifi · S. M. A. Nasab · M. Taghavi
Polymer Chemistry Research Laboratory, Department of Chemistry,
University of Mazandaran, Babolsar 47416-95447, Islamic Republic of Iran
e-mail: ghaemy@umz.ac.ir

outstanding solvent resistance [1–8]. However, these polymers usually present limited solubility and high melting temperatures, which decrease their processability and restrict further applications. Therefore, researches have been focused on the development of structurally modified aromatic polyamides with increased solubility and better processability [9–12]. Aromatic polymers that contain aryl ether or aryl sulfone linkages because of lower energy of internal rotation generally have lower glass-transition temperature (T_g), greater chain flexibility, and greater tractability than their corresponding polymers without these groups in the repeat units [13–23]. One of the successful approaches is the introduction of bulky aromatic heterocyclic pendants such as substituted imidazole and carbazole rings into the polymer backbone [24–27], which have also been suggested as promising photoconductive and photorefractive materials [28–33]. The rigidity, symmetry, and aromaticity of these systems contribute to thermal and chemical stability and enhanced mechanical properties of the resulting polymer at elevated temperatures; in addition, increase of polarizability of the nitrogen atom in the heterocyclic ring by introducing phenyl groups, such as 2,4,6-triarylimidazole, improves the solubility of the polymer in organic solvents [34–37].

In this paper, we wish to report synthesis of novel high-performance and processible poly(amide-ether)s (PAEs) with unique properties of solubility, thermal stability, and optical characteristics. New symmetric diamines containing two 3,4-diphenyl imidazole rings and flexible ether linkages, bis(4-(4-amino-2-(4,5-diphenyl-1H-imidazol-2-yl)phenoxy)phenyl)methanone and bis(4-(4-amino-2-(4,5-diphenyl-1H-imidazol-2-yl)phenoxy)phenyl)hexafluoropropane were synthesized and used for preparation of PAEs. The combination of functional groups of flexible, symmetrical, and bulky pendants in the backbone of these polymers will be expected to decrease the regularity of polymer chains, weaken the intermolecular interactions and chain packing efficiency, increase the barrier for free rotation and T_g , and thermal stability. Also, the introduction of 2,4,6-triarylimidazole (lophine) into the polymer backbone and the effects of induction and resonant electron groups on the properties of these polymers are investigated.

Experimental

Materials

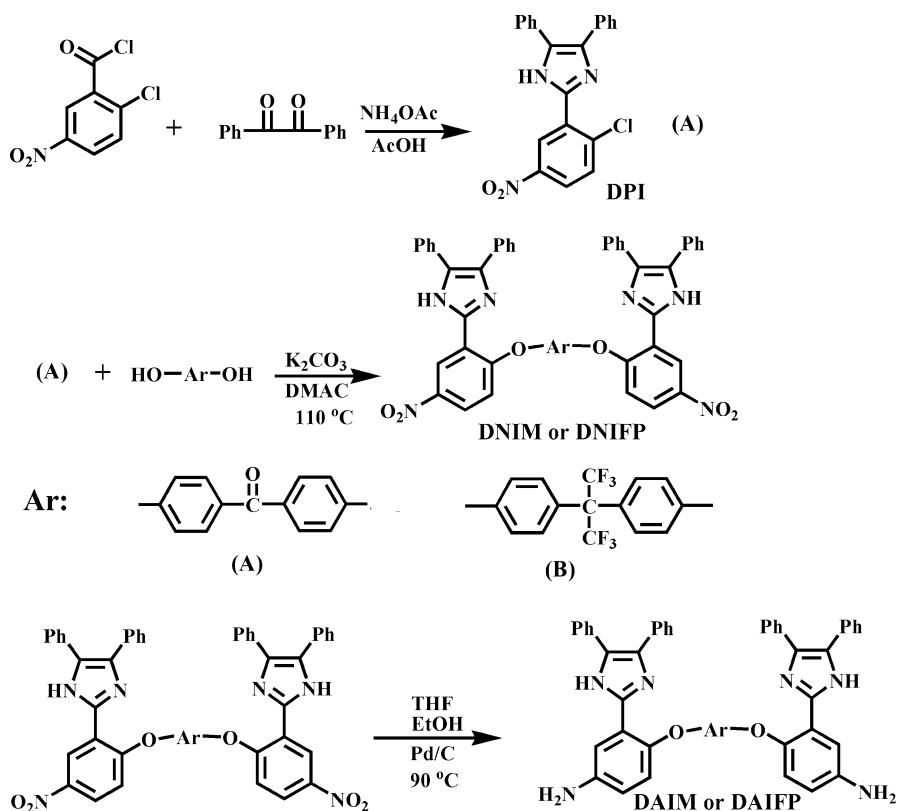
All chemicals were purchased from Fluka and Merck Chemical Co. (Germany) through a local agency. Ammonium acetate, hydrazine monohydrate, and 10 % palladium on activated carbon were used as received. NMP, DMAc, and pyridine (Py) were purified by distillation under reduced pressure over calcium hydride and stored over 4 Å molecular sieves.

Monomer synthesis

The synthetic pathway leading to the synthesis of target diamines is outlined in Scheme 1.

Synthesis of 2-(2-chloro-5-nitrophenyl)-4,5-diphenyl-1H-imidazole (DPI)

In a 250 mL round-bottomed two-necked flask equipped with a condenser, a magnetic stirrer bar and a nitrogen gas inlet tube, a mixture of 1.86 g (0.01 mol) 2-chloro-5-nitrobenzaldehyde, 2.1 g (0.01 mol) benzil, 5.39 g (0.07 mol) ammonium acetate, and 20 mL of glacial acetic acid was refluxed for 24 h. Upon cooling, the precipitated white solid was collected by filtration and washed with mixture of C₂H₅OH/H₂O (50/50, v/v). 3.55 g (yield 95 %) yellow crystals were obtained with the melting point (mp) 218–220 °C. FT-IR (KBr) at cm⁻¹: 3453 (N–H), 3124 (C–H aromatic), 1684 (C–N), 1532 and 1345 (NO₂). ¹H NMR (DMSO-*d*₆, δ in ppm): 7.34–7.39 (m, 6H, Ar–H), 7.54 (d, 4H, Ar–H, *J* = 8.2 Hz), 7.91 (d, 1H, Ar–H, *J* = 8.2 Hz), 8.25 (dd, 1H, Ar–H, *J* = 8.2 Hz), 8.65 (d, 1H, Ar–H, *J* = 2.8 Hz), 12.98 (s, 1H, N–H imidazole ring). Elemental analysis calculated for C₂₁H₁₄ClN₃O₂: C, 67.20; H, 3.73; N, 11.20. Found: C, 67.00; H, 3.65; N, 11.35.



Scheme 1 Synthesis of target diamines

Synthesis of bis(4-(4-nitro-2-(4,5-diphenyl-1H-imidazol-2-yl)phenoxy)phenyl)methanone (DNIM)

In a 250 mL round-bottomed two-necked flask equipped with a condenser, a magnetic stirrer bar and a nitrogen gas inlet tube, a mixture of 1.10 g (0.005 mol) 4,4'-dihydroxybenzophenone, 3.75 g (0.01 mol) (DPI), and 1.40 g (0.01 mmol) anhydrous potassium carbonate in 20 mL of dry DMAc was refluxed at 120 °C for 12 h and then cooled. The mixture was then poured into water and the precipitate was collected by filtration and recrystallized from ethanol. The yield of the crude product was 4.10 g (92 %), mp = 295–298 °C. FT-IR (KBr disk) at cm^{-1} : 3453 (NH), 3079 (C–H aromatic), 1608 (C=N), 1588 (C=C), 1532, 1350 (NO_2), and 1264 (C–O–C). ^1H NMR ($\text{DMSO-}d_6$, δ in ppm): 6.93 (distorted s, 2H, Ar–H), 7.22–7.34 (m, 16H, Ar–H), 7.46–7.57 (m, 12H, Ar–H), 7.89 (distorted s, 2H, Ar–H), 8.06 (d, 2H, Ar–H, $J = 8.2$ Hz), 13.33 (s, 2H, N–H imidazole ring). Elemental analysis calculated for $\text{C}_{55}\text{H}_{36}\text{N}_6\text{O}_7$: C, 74.00 %; H, 4.04 %; N, 9.42 % and found: C, 73.91 %; H, 4.15 %; N, 9.41 %.

Synthesis of bis(4-(4-nitro-2-(4,5-diphenyl-1H-imidazol-2-yl)phenoxy)phenyl)hexafluoropropane (DNIFP)

In a 250 mL round-bottomed two-necked flask equipped with a condenser, a magnetic stirrer bar and a nitrogen gas inlet tube, a mixture of 1.68 g (0.005 mol) 4,4'-(hexafluoroisopropylidene) diphenol, 3.75 g (0.01 mol) (DPI), and 1.40 g (0.01 mmol) anhydrous potassium carbonate in 20 mL of dry DMAc was refluxed at 120 °C for 12 h and then cooled. The mixture was then poured into water and the precipitate was collected by filtration and recrystallized from ethanol. The yield of the crude product was 4.70 g (94 %), mp = 278–280 °C. FT-IR (KBr disk) at cm^{-1} : 3484, 3378 (NH_2), 3445 (N–H imidazole ring), 3049 (C–H aromatic), 1633 (C=N), 1598 (C=C), 1530, 1351 (NO_2), and 1208 (C–O–C). ^1H NMR ($\text{DMSO-}d_6$, δ in ppm): 6.55 (distorted s, 2H, Ar–H), 7.04 (d, 4H, Ar–H, $J = 8$ Hz), 7.19–7.23 (m, 6H, Ar–H), 7.26–7.29 (m, 9H, Ar–H), 7.31–7.34 (m, 5H, Ar–H), 7.49 (d, 4H, Ar–H, $J = 8$ Hz), 7.90 (d, 4H, Ar–H, $J = 8$ Hz), 9.98 (s, 2H, N–H imidazole ring). Elemental analysis calculated for $\text{C}_{57}\text{H}_{36}\text{F}_6\text{N}_6\text{O}_6$: C, 67.46 %; H, 3.55 %; N, 8.28 % and found: C, 67.39 %; H, 3.64 %; N, 8.25 %.

Synthesis of bis(4-(4-amino-2-(4,5-diphenyl-1H-imidazol-2-yl)phenoxy)phenyl)methanone (DAIM)

To a 250 mL round-bottomed three-necked flask equipped with a dropping funnel, a reflux condenser, and a magnetic stirrer bar, 4.45 g (0.005 mol) bis(4-(4-nitro-2-(4,5-diphenyl-1H-imidazol-2-yl)phenoxy)phenyl)methanone (DNIM) and 0.1 g palladium on activated carbon (Pd/C, 10 %) were dispersed in 30 mL ethanol. The suspension solution was heated to reflux, and 5 mL of hydrazine monohydrate was added slowly to the mixture. After a further 8 h of reflux, the solution was filtered hot to remove Pd/C, and the filtrate was cooled to give white crystals. The product was collected by filtration and dried in vacuum at 80 °C. The yield of the reaction was

84 % (3.5 g), mp = 232–235 °C. FT-IR (KBr disk) at cm^{-1} : 3474, 3334 (NH_2), 3448 (N–H imidazole ring), 3035 (C–H aromatic), 1612 (C=N), 1498 (C=C), and 1241 (C–O–C). ^1H NMR ($\text{DMSO}-d_6$, δ in ppm): 4.32 (s, 2H, N–H), 4.39 (s, 2H, N–H), 6.11 (d, 1H, Ar–H, $J = 2.8$ Hz), 6.24 (d, 1H, Ar–H, $J = 2.4$ Hz), 6.49 (dd, 2H, Ar–H, $J = 8$ Hz), 6.51 (dd, 2H, Ar–H, $J = 8$ Hz), 6.65 (d, 1H, Ar–H, $J = 8$ Hz), 6.67 (d, 1H, Ar–H, $J = 8$ Hz), 7.00 (d, 2H, Ar–H, $J = 8$ Hz), 7.15 (d, 2H, Ar–H, $J = 8$ Hz), 7.17–7.41 (m, 20H, Ar–H), 7.43 (d, 4H, Ar–H, $J = 8$ Hz), 7.48 (d, 2H, Ar–H, $J = 8$ Hz), 10.97 (s, 1H, N–H imidazole ring), 11.54 (s, 1H, N–H imidazole ring). ^{13}C NMR (100 MHz, $\text{DMSO}-d_6$, δ in ppm): 113.93, 114.63, 117.37, 117.94, 124.59, 126.63, 128.86, 129.26, 130.12, 130.67, 130.72, 131.65, 132.75, 133.94, 135.46, 138.14, 140.48, 141.41, 145.49, 147.70, 148.41, 198.40. Elemental analysis calculated for $\text{C}_{55}\text{H}_{40}\text{N}_6\text{O}_3$: C, 79.33 %; H, 4.81 %; N, 10.09 % and found: C, 79.21 %; H, 4.96 %; N, 10.05 %.

Synthesis of bis(4-(4-amino-2-(4,5-diphenyl-1H-imidazol-2-yl)phenoxy)phenyl)hexafluoropropane (DAIFP)

To a 250 mL round-bottomed three-necked flask equipped with a dropping funnel, a reflux condenser, and a magnetic stirrer bar, 5.00 g (0.005 mol) bis(4-(4-nitro-2-(4,5-diphenyl-1H-imidazol-2-yl)phenoxy)phenyl) hexafluoropropane (DNIFP) and 0.1 g palladium on activated carbon (Pd/C, 10 %) were dispersed in 50 mL ethanol. The suspension solution was heated to reflux, and 7 mL of hydrazine monohydrate was added slowly to the mixture. After a further 8 h of reflux, the solution was filtered hot to remove Pd/C, and the filtrate was cooled to give white crystals. The product was collected by filtration and dried in vacuum at 80 °C. The yield of the reaction was 86 % (4.1 g), mp = 200–204 °C. FT-IR (KBr disk) at cm^{-1} : 3481, 3382 (NH_2), 3458 (N–H imidazole ring), 3051 (C–H aromatic), 1614 (C=N), 1498 (C=C), and 1247 (C–O–C). ^1H NMR ($\text{DMSO}-d_6$, δ in ppm): 4.30 (s, 4H, N–H), 6.16 (d, 2H, Ar–H, $J = 2.8$ Hz), 6.52 (dd, 2H, Ar–H, $J = 8$ Hz), 6.65 (d, 2H, Ar–H, $J = 8$ Hz), 7.14 (d, 4H, Ar–H, $J = 8.4$ Hz), 7.19–7.34 (m, 20H, Ar–H), 7.47 (d, 4H, Ar–H, $J = 8.4$ Hz), 10.80 (s, 2H, N–H imidazole ring). Elemental analysis calculated for $\text{C}_{57}\text{H}_{40}\text{F}_6\text{N}_6\text{O}_2$: C, 71.70 %; H, 4.19 %; N, 8.81 % and found: C, 71.62 %; H, 4.29 %; N, 8.76 %.

Polymer synthesis

The following general procedure, as is illustrated in Scheme 2, was used for the preparation of all PAEs from the diamines and various aliphatic and aromatic dicarboxylic acids. The new diamines (1 mmol), a dicarboxylic acid (1 mmol), and lithium chloride (0.30 g) were dissolved in a mixture of pyridine (1 mL), triphenylphosphite (TPP) (1.20 mmol), and NMP (5 mL) in a three-necked flask equipped with a condenser, a mechanical stirrer, and a nitrogen gas inlet tube. The mixture was heated at 120 °C for 12 h with stirring under dry N_2 atmosphere. The reaction mixture was then cooled to room temperature and the resulting polymers were precipitated in 200 mL methanol. The precipitate was filtered and washed with hot water, and then was further purified by washing with methanol for 1 day in a

Soxhlet apparatus to remove the low-molecular weight fractions. The inherent viscosity (η_{inh}) of the polymers measured at a concentration 0.5 g/dL in NMP at 25 °C were in the range of 0.41–0.65 dL/g.

PAEa1

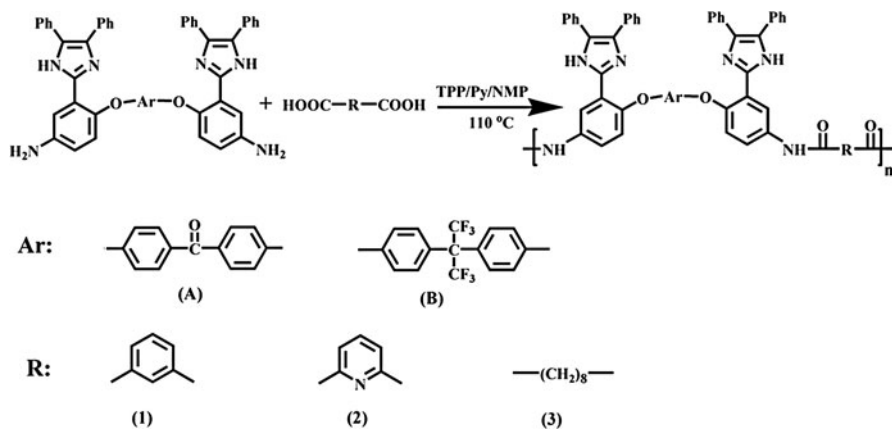
Yield 90 % and η_{inh} (dL/g) = 0.65. FT-IR (KBr disk) at cm^{-1} : 3347 (N–H amide), 3060 (C–H aromatic), 1654 (C=O amide), 1603 (C=N), 1552 (C=C) and 1249 (C–O–C). ^1H NMR (400 MHz, DMSO- d_6 , δ in ppm): 6.91–8.39 (m, 38H, Ar–H), 10.14 (s, 2H, N–H amide), 13.08 (s, 2H, N–H imidazole ring). Elemental analysis calculated for $(\text{C}_{63}\text{H}_{42}\text{N}_6\text{O}_5)_n$: C, 78.59 %; H, 4.37 %; N, 8.73 %. Found: C, 78.41 %; H, 4.42 %; N, 8.72 %.

PAEa2

Yield 87 % and η_{inh} (dL/g) = 0.48. FT-IR (KBr disk) at cm^{-1} : 3420 (N–H amide), 3035 (C–H aromatic), 1671 (C=O amide), 1605 (C=N), 1504 (C=C) and 1221 (C–O–C). ^1H NMR (400 MHz, DMSO- d_6 , δ in ppm): 7.11–8.28 (m, 33H, Ar–H), 10.14 (s, 2H, N–H amide), 12.93 (s, 2H, N–H imidazole ring). Elemental analysis calculated for $(\text{C}_{62}\text{H}_{41}\text{N}_7\text{O}_5)_n$: C, 77.26 %; H, 4.26 %; N, 10.18 %. Found: C, 77.11 %; H, 4.39 %; N, 10.18 %.

PAEa3

Yield 92 % and η_{inh} (dL/g) = 0.52. FT-IR (KBr disk) at cm^{-1} : 3422 (N–H amide), 3060 (C–H aromatic), 2923 (C–H aliphatic), 1675 (C=O amide), 1605 (C=N), 1500 (C=C) and 1243 (C–O–C). ^1H NMR (400 MHz, DMSO- d_6 , δ in ppm): 1.09 (m, 8H, C–H), 1.35 (m, 4H, C–H), 2.08 (t, 4H, C–H), 7.21–8.04 (m, 34H, Ar–H), 9.55 (s, 2H, N–H amide), 13.08 (s, 2H, N–H imidazole ring). Elemental analysis calculated



Scheme 2 Polycondensation reactions of the diamines with different dicarboxylic acids

for $(C_{65}H_{54}N_6O_5)_n$: C, 78.16 %; H, 5.41 %; N, 8.42 %. Found: C, 78.10 %; H, 5.48 %; N, 8.40 %.

PAEb1

Yield 92 % and η_{inh} (dL/g) = 0.61. FT-IR (KBr disk) at cm^{-1} : 3423 (N–H amide), 3035 (C–H aromatic), 1670 (C=O amide), 1604 (C=N), 1507 (C=C) and 1211 (C–O–C). 1H NMR (400 MHz, DMSO- d_6 , δ in ppm): 6.86–8.36 (m, 38H, Ar–H), 10.07 (s, 2H, N–H amide), 12.19 (s, 2H, N–H imidazole ring). Elemental analysis calculated for $(C_{65}H_{42}F_6N_6O_4)_n$: C, 71.96 %; H, 3.87 %; N, 7.75 %. Found: C, 71.85 %; H, 3.96 %; N, 7.72 %.

PAEb2

Yield 90 % and η_{inh} (dL/g) = 0.41. FT-IR (KBr disk) at cm^{-1} : 3425 (N–H amide), 3036 (C–H aromatic), 1669 (C=O amide), 1604 (C=N), 1507 (C=C) and 1229 (C–O–C). 1H NMR (400 MHz, DMSO- d_6 , δ in ppm): 6.99–8.27 (m, 33H, Ar–H), 10.15 (s, 2H, N–H amide), 12.92 (s, 2H, N–H imidazole ring). Elemental analysis calculated for $(C_{64}H_{41}F_6N_7O_4)_n$: C, 70.78 %; H, 3.78 %; N, 9.03 %. Found: C, 70.65 %; H, 3.82 %; N, 9.02 %.

PAEb3

Yield 95 % and η_{inh} (dL/g) = 0.49. FT-IR (KBr disk) at cm^{-1} : 3435 (N–H amide), 3024 (C–H aromatic), 2963 (C–H aliphatic), 1671 (C=O amide), 1604 (C=N), 1501 (C=C) and 1237 (C–O–C). 1H NMR (400 MHz, DMSO- d_6 , δ in ppm): 1.07 (m, 8H, C–H), 1.32 (m, 4H, C–H), 2.08 (t, 4H, C–H), 6.83–7.74 (m, 34H, Ar–H), 9.50 (s, 2H, N–H amide), 12.44 (s, 2H, N–H imidazole ring). Elemental analysis calculated for $(C_{67}H_{54}F_6N_6O_4)_n$: C, 71.78 %; H, 4.82 %; N, 7.50 %. Found: C, 71.72 %; H, 4.93 %; N, 7.48 %.

Measurements

Proton and carbon nuclear magnetic resonance (1H NMR and ^{13}C NMR) spectra were recorded on a 400 MHz Bruker (Ettlingen, Germany) instrument using DMSO- d_6 as solvent and tetramethyl silane as an internal standard. Elemental analyses performed by a CHN-600 Leco elemental analyzer. Melting point (uncorrected) was measured with a Barnstead Electrothermal Engineering Ltd 9200 apparatus. Inherent viscosities (at a concentration of 0.5 g/dL) were measured with an Ubbelohde suspended-level viscometer at 25 °C using NMP as solvent. Qualitative solubility was determined using 0.05 g of the polymer in 0.5 mL of solvent. Thermogravimetric analysis (TGA) was performed with the DuPont Instruments (TGA 951) analyzer well equipped with a PC at a heating rate of 10 °C/min under nitrogen atmosphere (20 cm^3 /min) and in the temperature range of 30–750 °C. Differential scanning calorimeter (DSC) was recorded on a Perkin-Elmer pyris 6 DSC under nitrogen atmosphere (20 cm^3 /min) at a heating rate of

10 °C/min. Glass-transition temperatures (T_g) values were read at the middle of the transition in heat capacity and were taken from the second heating scan after cooling from 350 °C at a cooling rate of 20 °C/min. Ultraviolet–visible and fluorescence emission spectra were recorded on a Cecil 5503 (Cecil Instruments, Cambridge, UK) and Perkin-Elmer LS-3B spectrophotometers (Norwalk, CT, USA) (slit width = 2 nm), respectively, using a dilute polymer solution (0.20 g/dL) in DMSO.

Results and discussion

Synthesis and characterization of diamines

The objective of this study was the preparation of novel thermally stable and organosoluble PAEs based on substituted pendent imidazole ring and ether linkage in the backbone of polymer. Condensation of benzil with 2-chloro-5-nitrobenzaldehyde and ammonium acetate is well known as a classical but convenient synthetic method for preparation of triaryl imidazole. After reaction, ^1H NMR spectrum of DPI showed a peak in the region of 12.98 ppm which is related to N–H of formation of imidazole ring. The dinitro compounds were successfully synthesized from DPI and diols as starting materials by the nucleophilic chlorodisplacement reaction according to the synthetic route shown in Scheme 1. The diamines were obtained by catalytic reduction of the intermediate dinitro compounds using hydrazine hydrate and Pd/C in refluxing ethanol. The structures of the dinitro and diamine compounds were identified by elemental analysis, FT-IR, and ^1H and ^{13}C NMR spectroscopy techniques. The nitro groups were evident from the FT-IR peaks at 1,530 and 1,350 cm^{-1} related to the symmetric and asymmetric stretching of NO_2 . After reduction, these absorption peaks disappeared and the primary amino group in diamine showed the typical absorption pair at 3,481 and 3,382 cm^{-1} . As shown in Fig. 1, the ^1H NMR spectrum of diamine (DAIFP) confirms that the nitro groups were completely transformed into the amine groups by the high-field shift of the aromatic protons. The ^1H NMR spectrum of this compound also showed the characteristic resonance of protons of amine groups at 4.30 ppm. The ^{13}C NMR spectrum of DAIM shows 22 different carbons for the aromatic segment and heterocyclic ring (Fig. 2).

Polymers synthesis and characterization

The new thermally stable PAEs were synthesized by phosphorylation polycondensation between the diamines and various commercially available aromatic and aliphatic dicarboxylic acids in NMP using TPP and pyridine as condensing agents at 120 °C in N_2 (Scheme 2). All the polycondensation reactions proceeded readily in a homogeneous solution. Since Yamazaki et al.'s [38] development, many researchers have utilized the activated polyamidation using the TPP activator and found that the addition of a small amount of LiCl or CaCl_2 enhances the molecular weight of the polyamides. Stringy and tough precipitates formed when the viscous polymer solutions were trickled into the stirring methanol. As shown in Table 1, the inherent viscosities of polymers were in the range of 0.41–0.65 dL/g. The elemental analysis

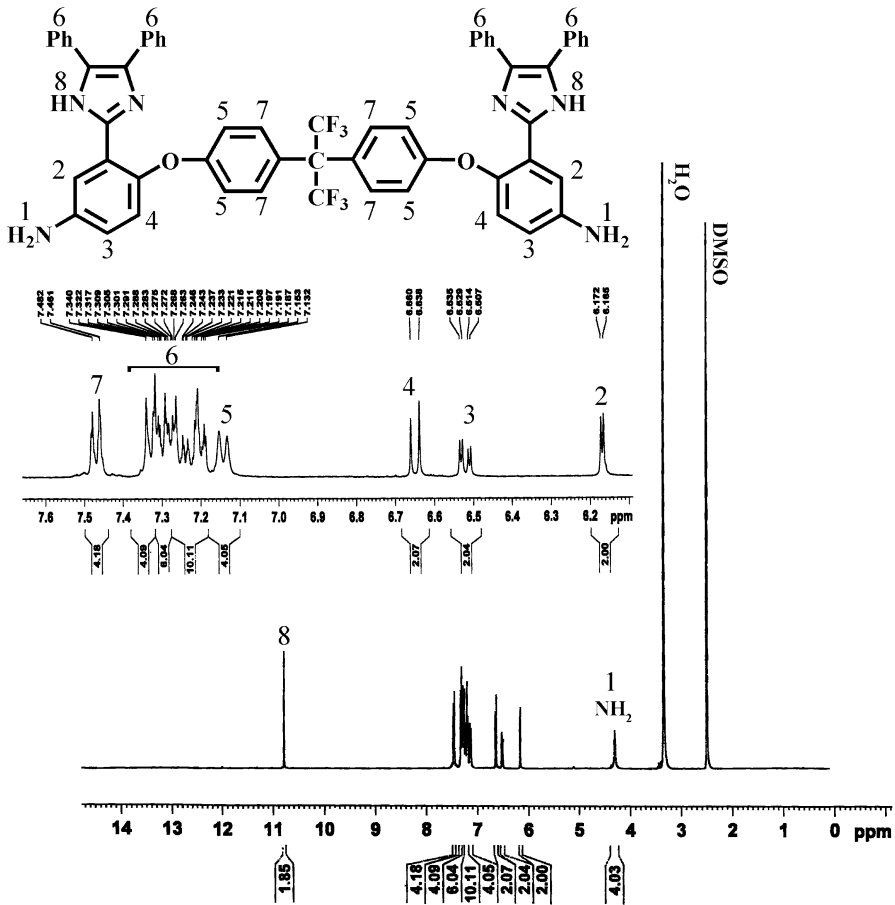


Fig. 1 ^1H NMR spectrum of diamine (DAIFP) in $\text{DMSO-}d_6$

values generally agreed with the calculated values for the proposed structures of polymers. Structural features of these PAEs were verified by FT-IR and ^1H NMR spectroscopy. FT-IR spectrum of the representative polymer PAEb3 is shown in Fig. 3. They exhibited characteristic absorption bands around $3,400\text{ cm}^{-1}$ (N–H stretch), near $1,250\text{ cm}^{-1}$ (aryl ether stretching) and at $1,665\text{ cm}^{-1}$ (C=O, amide). ^1H NMR spectrum of the representative polymer PAEb3 was illustrated in Fig. 4, where all the peaks could be readily assigned to the protons in the repeating unit. In the ^1H NMR spectra of these polymers, the N–H proton of amide groups appeared in the region of $9.50\text{--}10.15\text{ ppm}$, while the N–H proton of imidazole ring appeared at the most downfield region of 13.00 ppm .

Solubility of PAEs

The solubility behavior of these PAEs was qualitatively tested in various organic solvents, and the results are summarized in Table 1. All prepared PAEs exhibited

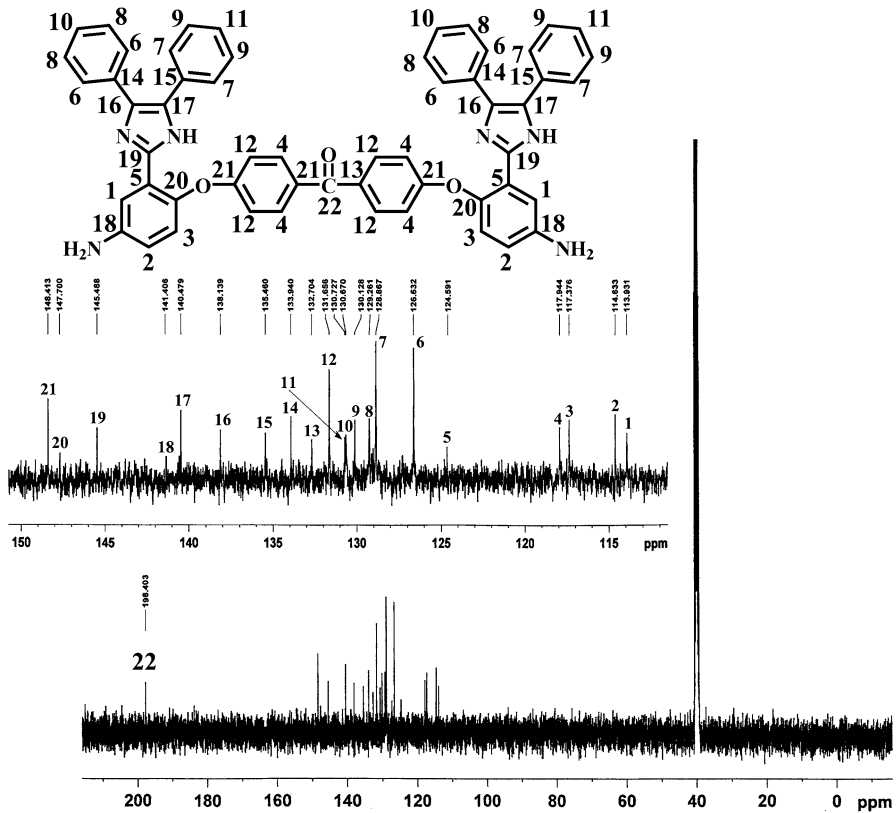


Fig. 2 ^{13}C NMR spectrum of diamine (DAIM) in $\text{DMSO-}d_6$

Table 1 Solubility of synthesized PAEs

Code	Solvent	Yield (%)	η_{inh} (dL/g) ^a								
				NMP	DMAc	NMP	DMSO	Py	THF	<i>m</i> -cresol	TCE
PAEa1	90	0.65	++	++	++	++	±	±	+	–	
PAEa2	87	0.48	++	++	++	++	±	±	+	–	
PAEa3	92	0.52	++	++	++	++	+	+	++	–	
PAEb1	92	0.61	++	++	++	++	+	+	+	±	
PAEb2	90	0.41	++	++	++	++	+	+	++	±	
PAEb3	95	0.49	++	++	++	++	++	+	++	±	

DMAc *N,N*-dimethyl acetamide, *DMF* *N,N*-dimethyl formamide, *NMP* *N*-methyl pyrrolidone, *DMSO* dimethyl sulfoxide, *Py* pyridine, *THF* tetrahydrofuran

++ soluble at room temperature, + soluble on heating at 80 °C, ± partially soluble on heating at 80 °C, – insoluble on heating at 80 °C

^a Measured at a polymer concentration of 0.5 g/dL in NMP at 25 °C

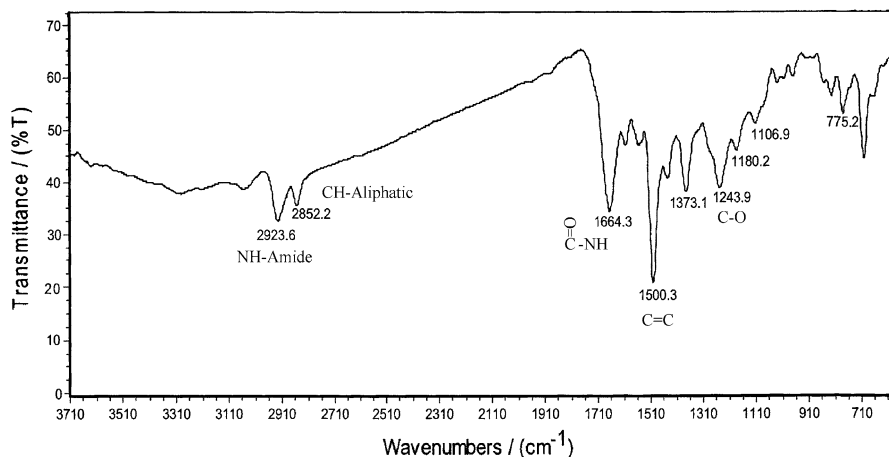


Fig. 3 FT-IR spectrum of PAEb3

excellent solubility in polar aprotic solvents such as NMP, DMAc, DMF, DMSO, and some of them in less polar solvents like pyridine and *m*-cresol at room temperature and in THF at high temperature. The good solubility should be the result of introduction of the bulky pendent diphenylimidazole group in polymer backbone. These factors increase the chain distance, inhibit the chain packing, and decrease the interaction of the polymer chains; consequently, the solvents molecules are able to penetrate easily and interact with the polar groups and to solubilize the polymer chains. The amorphous nature of the PAEs was also reflecting their good organosolubility. Besides the carbonyl and halogen groups have improved the solubility of these polymers. Among the PAEs, polymers containing CF_3 polar groups show better solubility in less polar and aliphatic solvents due to the presence of aliphatic section which results in the increment of the flexibility of the polymer structure. We believe, however, that the presence of imidazole and ether groups in the pendent and in the main chain, respectively, can also contribute effectively in the solubility of these PAEs by interacting with the polar molecules of solvents. In addition, the solubility varies depending upon the dicarboxylic acid used. PAEs were synthesized from aliphatic dicarboxylic acids (PAEa3 and PAEb3) exhibited better solubility behavior in less polar solvents such as THF and *m*-cresol. The methylene units instead of rigid phenyl improve the solubility of these polyamides.

UV–vis absorption and fluorescence characteristics

The UV–vis absorption and photoluminescence (PL) spectra of the diamines and PAEs in dilute (0.2 g/dL) NMP solution and for PAEs in films (thickness 50 μm) are shown in Figs. 5 and 6, and the data were summarized in Table 2. The diamines and PAEs exhibited strong UV–vis absorption bands with maxima at 300 nm and in the range of 302–315 nm, respectively, assignable to the π – π^* transition resulting from the aromatic moieties. By comparing spectra, a slightly red shift is observed in

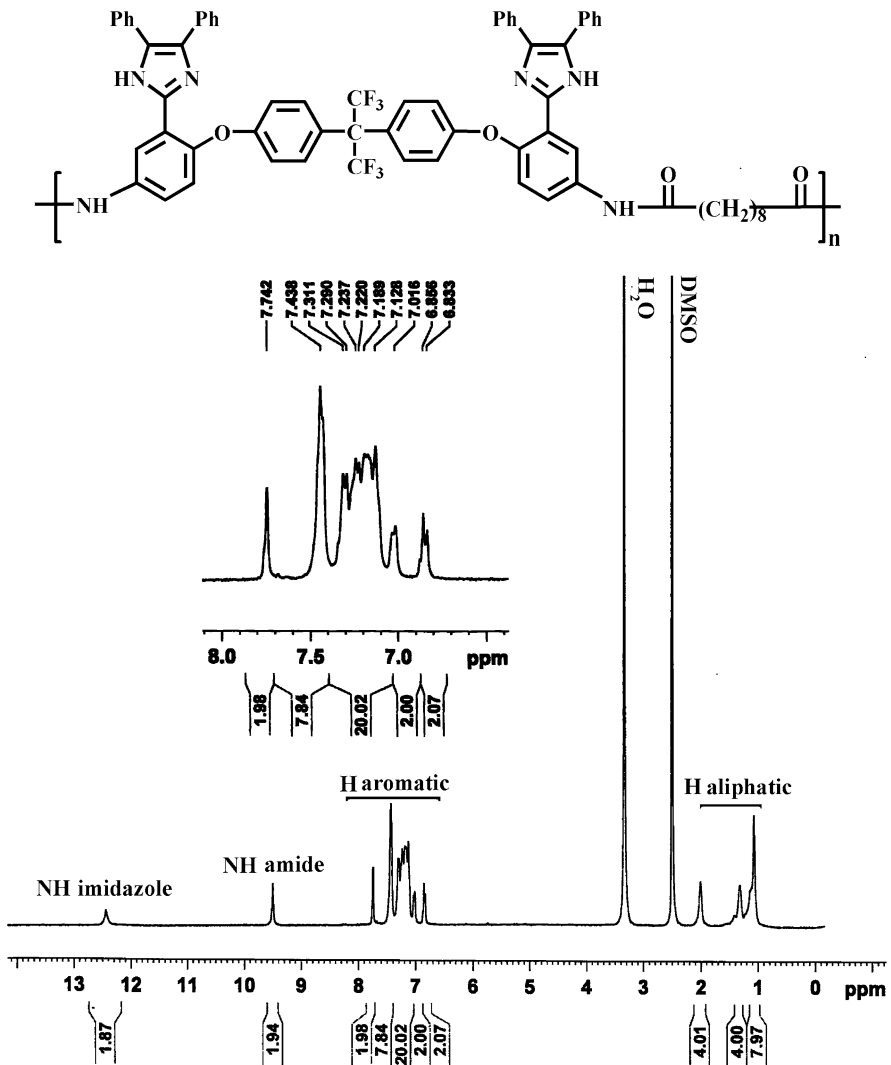


Fig. 4 ^1H NMR spectrum of PAEb3 in $\text{DMSO-}d_6$

PAEs spectra due to expansion of π system. To investigate the optical properties of thin films of these PAEs, solutions of the polymers were made by dissolving about 0.50 g of the samples in 6 mL of NMP. These solutions were poured into a 5-cm glass Petri dish, which was heated under vacuum at 50 °C for 1 h, 100 °C for 2 h, and 150 °C for 5 h to evaporate the solvent slowly. By being soaked in distilled water, the flexible and transparent thin films with almost no color was self-stripped off from the glass surface. The obtained films were then used to investigate the optical properties of the PAEs. The maximum emission ($\lambda_{\text{max}}(\text{em})$) of the diamines in NMP solution was observed at 395 nm for DAIM and 400 nm for DAIFP. The

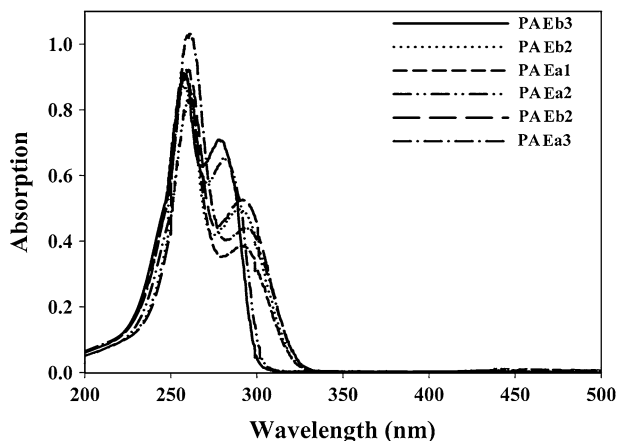


Fig. 5 UV-vis spectrum of PAEs in solution

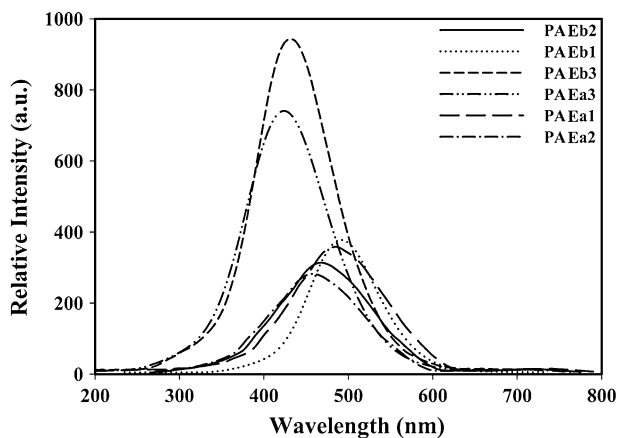


Fig. 6 Fluorescence spectrum of PAEs in film

PL spectra of PAEs in NMP solution and in films (thickness 50 μm) exhibited a high-intensity maximum around 456–492 nm for the aromatic PAEs (PAEa1, PAEb1, PAEa2, and PAEb2) and at 423–427 nm for the aliphatic PAEs (PAEa3 and PAEb3). To measure the PL quantum yields (Φ_f), dilute polymer solutions (0.2 g/dL) in NMP were prepared. A 0.1 N solution of quinine in H_2SO_4 ($\Phi_f = 0.55$) was used as reference according to the literature [39]. The Φ_f values were 0.30 for DAIM and 0.32 for DAIFP, 0.21 and 0.28 for the aliphatic PAEa3 and PAEb3, respectively, and in the range of 0.06–0.10 for the aromatic PAEs. The maximum emission wavelength and the Φ_f values of these polymers particularly PAEa3, PAEb1, and PAEb3 are comparable with the photophysical properties of materials reported by other researchers [40, 41]. The blue shift and higher fluorescence quantum yield of the aliphatic PAEs compared with the aromatic PAEs

Table 2 Optical properties data of PAEs

Polymer	λ_{abs} (nm) ^a	λ_{em} (nm) ^a	λ_{abs} (nm) ^b	λ_{em} (nm) ^b	Φ_f (%) ^c
PAEa1	313	484	315	486	8
PAEa2	310	456	310	457	6
PAEa3	305	423	308	426	21
PAEb1	315	492	316	494	10
PAEb2	312	469	314	470	7
PAEb3	307	427	308	431	28

Polymer concentration of 0.20 g/dL in NMP

^a UV–visible spectra of the PAEs in solution

^b Fluorescence spectra of the film

^c Fluorescence quantum yield relative to 0.1 N quinine sulfate in 1 N H₂SO₄ (aq) ($\Phi_f = 0.55$) as a standard

could be attributed to reduced conjugation and capability of charge-transfer complex formation by the aliphatic diacids with the electron-donating diamine moiety in comparison to the stronger electron-accepting aromatic diacids [42].

Thermal properties

DSC and TGA methods were applied to evaluate the thermal properties of the polymers. The DSC curves of the PAEs were recorded at heating rate of 10 °C/min in N₂ are shown in Fig. 7. Melting endothermic peak was not observed in the DSC curves of PAEs which emphasize the amorphous nature of these polymers. The amorphous nature of these PAEs can be attributed to their bulky pendent group which decreased the interchain interaction resulting in loose polymer chain packaging and aggregates. The T_g values were taken as the midpoint of the change in slope of the baseline of DSC curves, and found to be in the range of 204–308 °C, as shown in Table 3. The presence of flexible bond such as ether linkage in the main chain of these polymers reduced the rigidity of their backbones and consequently T_g of these polymers to a reasonable and obtainable values in the range of 204–308 °C. In general, molecular packing and chain rigidity are among the main factors influencing on T_g values. Therefore, T_g values of these polymers are affected by these two opposite key factors; bulky pendants and flexibility of the main chain by ether linkages. In general, the T_g values of PAEs containing CF₃ aliphatic group is lower than that of those containing carbonyl group which can be assigned to the symmetric and as a result of better flexibility of CF₃ groups. The T_g values also depend on the flexibility of the diacid residue in the polymer main chain. Therefore, among all the synthesized PAEs, the PAEa3 and PAEb3 based on aliphatic dicarboxylic acid showed the lowest T_g values and those based on the aromatic dicarboxylic acids such as PAE (a1, a2, b1, and b2) exhibited the highest T_g values.

Thermal stability of these polymers was evaluated by TGA in N₂ atmosphere and the curves are shown in Fig. 8. The data, extracted from the original TGA curves, in Table 3, show the temperature of 10 % weight loss in the range of 330–450 °C in

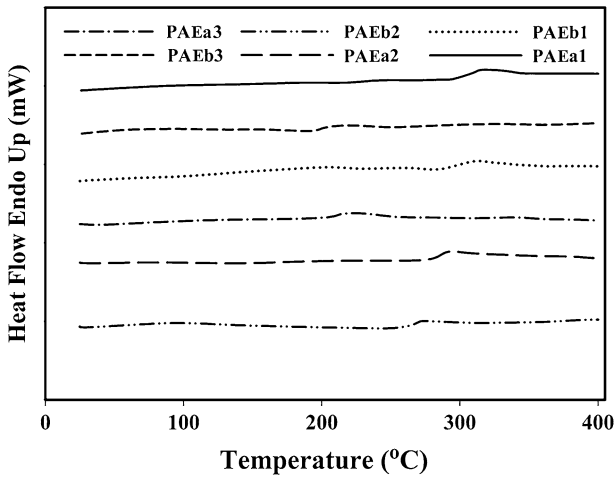


Fig. 7 DSC curves of PAE under a nitrogen atmosphere at a heating rate of 10 °C/min

Table 3 Thermal properties of PAEs

Polymer	T_5 (°C) ^a	T_{10} (°C) ^b	T_g (°C) ^c	Char yield ^d	LOI (%) ^e
PAEa1	387	450	308	63	43
PAEa2	301	360	287	55	40
PAEa3	290	336	211	41	34
PAEb1	339	401	299	59	41
PAEb2	295	343	264	48	37
PAEb3	284	330	204	29	29

^a Temperature at which 5 % weight loss was recorded by TGA at a heating rate of 10 °C/min in a nitrogen atmosphere

^b Temperature at which 10 % weight loss was recorded by TGA at a heating rate of 10 °C/min, in a nitrogen atmosphere

^c Glass-transition temperature was recorded at a heating rate of 10 °C/min in a nitrogen atmosphere

^d Percentage weight of material left undecomposed after TGA analysis at a temperature of 750 °C in a nitrogen atmosphere

^e Limiting oxygen index percent evaluating at char yield 750 °C

N_2 atmosphere. The residual weights for the resulting PAEs were in the range of 29–63 % at 750 °C in N_2 . Char yield can be used as criteria for evaluating limiting oxygen index (LOI) of the polymers in accordance with Van Krevelen and Hoftyzer equation [43]. $LOI = 17.5 + 0.4 CR$, where CR is the char yield. For all the PAEs, LOI values were calculated based on their char yields at 750 °C. Due to the reasons which have been explained above, the thermal stability of these PAEs are observed in order of PAEa > PAEb. According to Table 3, it is clear that aromatic PAEs have better thermal stability and higher LOI as compared to the aliphatic PAEs. This can be pertained to the rigid structure of aromatic diacids compared to the flexible

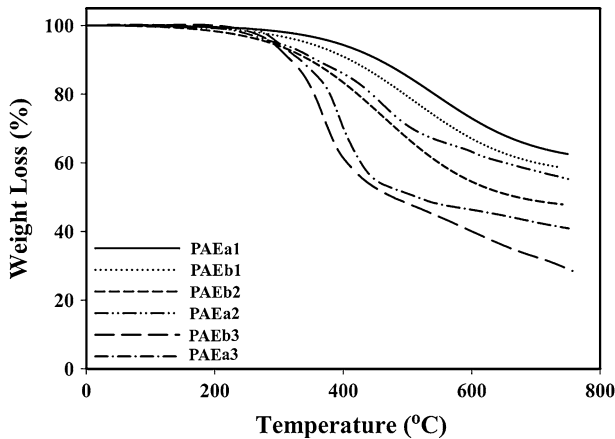


Fig. 8 TGA curves of PAE under a nitrogen atmosphere at a heating rate of 10 °C/min

structure of aliphatic diacids. The thermal resistance of polymers containing aliphatic CF_3 groups is less than those containing carbonyl group.

Conclusion

In this study, a series of novel photoactive PAEs containing bulky imidazole pendent groups and aryl ether linkages in the backbone have been successfully prepared by direct phosphorylation polycondensation of new diamines with various aromatic and aliphatic dicarboxylic acids. The introduction of combination of two flexible ether linkages and bulky triarylimidazole pendent groups into the polymer repeating units significantly improved the solubility of the prepared PAEs in various organic solvents. Most of these PAEs exhibited a desired combination of properties such as good solubility and moderate T_g values suitable for processing, good thermal stability with the ability of fluorescence emission necessary for high-performance materials.

References

1. García JM, García FC, Serna F, de la Peña JL (2010) High-performance aromatic polyamides. *Prog Polym Sci* 5:623–686
2. Hearle JW (2001) High-performance fibres. Woodhead Publishing Ltd., Cambridge
3. Gaudiana RA, Minns RA, Sinta R, Weeks N, Rogers HG (1989) Amorphous rigid-rod polymers. *Prog Polym Sci* 14:47–89
4. Cassidy PE (1980) Thermally stable polymers. Marcel Dekker, New York
5. Marchildon K (2011) Polyamides-still strong after seventy years. *Macromol React Eng* 5:22–54
6. Imai Y (1996) Recent advances in synthesis of high-temperature aromatic polymers. *React Funct Polym* 30:3–15
7. Mark HF (2004) Encyclopedia of polymer science and technology. Wiley, New York

8. Jeong HJ, Oishi Y, Kakimoto M, Imai Y (1990) Synthesis and characterization of novel aromatic polyamides from 3,4-bis(4-aminophenyl)-2,5-diphenylfuran and aromatic diacid chlorides. *J Polym Sci Polym Chem Ed* 28:3293–3301
9. Hsiao SH, Lin KH (2004) Soluble aromatic polyamides bearing asymmetrical diaryl ether groups. *Polymer* 45:7877–7885
10. Kricheldorf HR, Bohme S, Schwarz G (2001) Macrocycles the role of cyclization in kinetically controlled polycondensations polyamides. *Macromolecules* 34:8879–8885
11. Liou GS, Hsiao SH, Ishida M, Kakimoto M, Imai Y (2002) Synthesis and characterization of novel soluble triphenylamine-containing aromatic polyamides based on N, N'-bis(4-aminophenyl)-N, N'-diphenyl-1,4-phenylenediamine. *J Polym Sci A* 40:2810–2818
12. Ghaemy M, Porazizollahy R, Bazzar M (2011) Novel thermal stable organosoluble polyamides and polyimides based on quinoxalin bulky pendent group. *Macromol Res* 19:528–536
13. Bottino FA, Di Pasquale G, Pollicino A, Scalia L (1998) Synthesis and characterization of new polyamides containing 6,6'-methylenediquinoline units. *Polymer* 20:4949–4954
14. Zulficar S, Ahmad Z, Sarwar M (2007) Soluble aromatic polyamide bearing ether linkages: synthesis and characterization. *Colloid Polym Sci* 285:1749–1754
15. Ghaemy M, Hashemi Nasr F (2012) Synthesis of high performance polyamides utilizing copper-catalyzed amidation of a dibromoarene with different diamides. *J Appl Polym Sci* 124:1707–1715
16. Liaw DJ, Liaw BY, Kang ET (1999) Synthesis and characterization of new cardo polyamide-imides containing ether and tricyclo[5.2.1.0₂,6]decane groups. *Macromol Chem Phys* 200:2402–2406
17. Liaw DJ, Liaw BY (1998) Synthesis and characterization of new soluble polyamides containing ether and pendant cyclododecyldiene groups. *Polym Adv Technol* 9:740–745
18. Imai Y, Maldar NN, Kakimoto M (1985) Synthesis and characterization of soluble aromatic polyamides from 2,5-bis(4-aminophenyl)-3,4-diphenylthiophene and aromatic diacid chlorides. *J Polym Sci Polym Chem Ed* 23:1797–1803
19. In I, Kim SY (2006) Soluble wholly aromatic polyamides containing unsymmetrical pyridyl ether linkages. *Polymer* 47:547–552
20. Yu Y, Cai M, Zhang Y (2010) Study on synthesis of novel soluble aromatic polyamides with pendant cyano groups. *Polym Bull* 65:309–318
21. Li PH, Wang CY, Li G, Jiang JM (2010) Synthesis and characterization of novel polyamides derived from 1,4-bis((4-amino-2-(trifluoromethyl)phenoxy)methyl)cyclohexane and aromatic dicarboxylic acids. *Polym Bull* 64:127–140
22. Mallakpour S, Dinari M (2009) Preparation of thermally stable and optically active organosoluble aromatic polyamides containing L-leucine amino acid under green conditions. *Polym Bull* 63:623–635
23. Jiang JW, Pei XL, Sheng SR, Wu XY, Liu XL, Song CS (2011) Novel soluble fluorine-containing polyamides derived from 2-(4-trifluoromethylphenoxy)terephthalic acid and trifluoromethyl-substituted aromatic bis(ether amine)s. *Polym Bull* 67:263–274
24. Ghaemy M, Amini Nasab SM (2010) Synthesis and identification of organosoluble polyamides bearing a triaryl imidazole pendent: thermal, photophysical, chemiluminescent, and electrochemical characterization with a modified carbon nanotube electrode. *React Funct Polym* 70:306–313
25. Ghaemy M, Alizadeh R (2011) Synthesis, characterization and photophysical properties of organosoluble and thermally stable polyamides containing pendent N-carbazole group. *React Funct Polym* 71:425–432
26. Ghaemy M, Amini Nasab SM, Alizadeh R (2010) Synthesis and characterization of new soluble polyamides from an unsymmetrical diamine bearing a bulky triaryl pyridine pendent group. *J Appl Polym Sci* 116:3725–3731
27. Ghaemy M, Alizadeh R (2009) Synthesis of soluble and thermally stable polyimides from unsymmetrical diamine containing 2,4,5-triaryl imidazole pendent group. *Eur Polym J* 45:1681–1688
28. Kim HC, Kim JS, Kim KS, Park HK, Baek S, Ree M (2004) Synthesis and characterization of new, soluble polyazomethines bearing fluorene and carbazole units in the backbone and solubility-improving moieties in the side group. *J Polym Sci A* 42:825–834
29. Grigalevicius S, Grazulevicius JV, Gaidelis V, Jankauskas V (2002) Synthesis and properties of poly(3,9-carbazole) and low-molar-mass glass-forming carbazole compounds. *Polymer* 43:2603–2608
30. Grazulevicius JV, Strohrriegl P, Pieliowski J, Pieliowski K (2003) Carbazole-containing polymers: synthesis, properties and applications. *Prog Polym Sci* 28:1297–1353

31. Angiolini L, Giorgini L, Li H, Golemme A, Mauriello F, Termine R (2010) Synthesis, characterization and photoconductive properties of optically active methacrylic polymers bearing side-chain 9-phenylcarbazole moieties. *Polymer* 51:368–377
32. Hsiao SH, Chang YH (2004) New soluble aromatic polyamides containing ether linkages and laterally attached *p*-terphenyls. *Eur Polym J* 40:1749–1757
33. Tundidor-Camba A, Terraza CA, Tagle LH, Coll D (2011) Polyamides obtained by direct polycondensation of 4-[4-[9-[4-(4-aminophenoxy)-3-methyl-phenyl] fluoren-9-yl]-2-methyl-phenoxy]aniline with dicarboxylic acids based on a diphenyl-silane moiety. *J Appl Polym Sci* 120:2381–2389
34. Ghaemy M, Amini Nasab SM (2011) Synthesis and characterization of organo-soluble polyamides containing triaryl imidazole pendant and ether linkage moieties: thermal, photophysical, and chemiluminescent properties. *Polym Adv Technol* 22:2311–2318
35. Amini Nasab SM, Ghaemy M (2011) Synthesis and characterization of new polyamides and polyimides containing dioxypyrimidine moiety in the main chain with bulky imidazole pendent group: solubility, thermal and photophysical properties. *J Polym Res* 18:1575–1586
36. Ghaemy M, Alizadeh R, Behmadi H (2009) Synthesis of soluble and thermally stable polyimide from new diamine bearing *N*-[4-(9H-carbazol-9-yl)phenyl] formamide pendent group. *Eur Polym J* 45:3108–3115
37. Ghaemy M, Amini Nasab SM (2010) Synthesis and identification of organosoluble polyimides: thermal, photophysical and chemiluminescence properties. *Polym J* 42:648–656
38. Yamazaki N, Matsumoto M, Higashi F (1975) Studies on reactions of the *N*-phosphonium salts of pyridines. XIV. Wholly aromatic polyamides by the direct polycondensation reaction by using phosphites in the presence of metal salts. *J Polym Sci Polym Chem Ed* 13:1373–1380
39. Feng K, Hsu FL, Van DerVeer D, Bota K, Bu XR (2004) Tuning fluorescence properties of imidazole derivatives with thiophene and thiazole. *J Photochem Photobiol A* 165:223–228
40. Liou GS, Hsiao SH, Huang NK, Yang YL (2006) Photophysical, and electrochromic characterization of wholly aromatic polyamide blue-light-emitting materials. *Synthesis* 39:5337–5346
41. Fridman N, Kaftory M, Speiser S (2007) Structures and photophysics of lophine and double lophine derivatives. *Sens Actuat B* 126:107–115
42. Liou GS, Chang CW (2008) Highly stable anodic electrochromic aromatic polyamides containing *N,N,N'*-tetraphenyl-*p*-phenylenediamine moieties: synthesis, electrochemical, and electrochromic properties. *Macromolecules* 41:1667–1674
43. Van Krevelen DW (2008) Properties of polymers, 4th edn. Elsevier Scientific Publishing, Amsterdam